

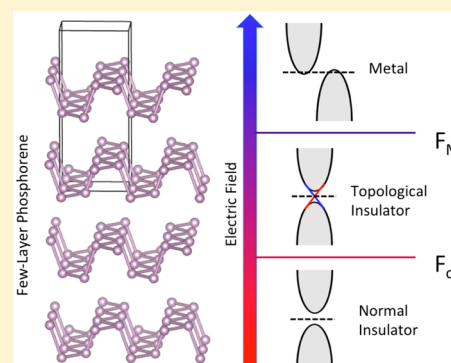
Switching a Normal Insulator into a Topological Insulator via Electric Field with Application to Phosphorene

Qihang Liu,^{*,†} Xiuwen Zhang,[†] L. B. Abdalla,[‡] Adalberto Fazzio,[‡] and Alex Zunger^{*,†}[†]University of Colorado, Boulder, Colorado 80309, United States[‡]Instituto de Física, Universidade de São Paulo, Butantã, São Paulo 05508, Brazil

ABSTRACT: The study of topological insulators has generally involved search of materials that have this property as an *innate quality*, distinct from normal insulators. Here we focus on the possibility of converting a normal insulator into a topological one by application of an external electric field that shifts different bands by different energies and induces a specific band inversion, which leads to a topological state. Phosphorene is a two-dimensional (2D) material that can be isolated through mechanical exfoliation from layered black phosphorus, but unlike graphene and silicene, single-layer phosphorene has a large band gap (1.5–2.2 eV). Thus, it was unsuspected to exhibit band inversion and the ensuing topological insulator behavior. Using first-principles calculations with applied perpendicular electric field F_{\perp} on few-layer phosphorene we predict a continuous transition from the normal insulator to a topological insulator and eventually to a metal as a function of F_{\perp} . The tuning of topological behavior with electric field would lead to spin-separated, gapless edge states, that is, quantum spin Hall effect.

This finding opens the possibility of converting normal insulating materials into topological ones via electric field and making a multifunctional “field effect topological transistor” that could manipulate simultaneously both spin and charge carrier. We use our results to formulate some design principles for looking for other 2D materials that could have such an electrical-induced topological transition.

KEYWORDS: phosphorene, topological insulator, spin hall transistor, electric field, black phosphorus, density functional theory



Although both topological insulators (TIs) and normal insulators (NIs) have finite band gap E_g separating the occupied from the unoccupied energy bands, materials that are TIs have, in addition band inversion between certain conduction and valence band states,¹ been characterized by a negative “inversion energy” Δ_{inv} and conveniently diagnosed by the topological invariant quantity² Z_2 being 1 rather than 0. Consequently, the $(N - 1)$ -dimensional version (2D surfaces or 1D edges) of such N -dimensional bulk TIs (respectively, 3D crystals or 2D layered crystals) manifest linearly dispersed crossing bands termed “Dirac cone” having opposite spin currents that are resilient to nonmagnetic chemical passivation and backscattering.^{2,3} Although most studies on TI and NI materials tend to focus on separate systems each having its own, fixed Δ_{inv} —either negative (a TI with $Z_2 = 1$) or positive (a NI with $Z_2 = 0$)—it would appear interesting as well as practically useful to realize a NI-to-TI topological phase transition in a single system by manipulating some type of continuous “knob”. This might be important for converting materials that are normally NIs to TIs, thus expanding the rather limited material base of TIs. Identifying such a NI-to-TI switch would be in particular interesting in 2D layered systems for establishing the device-relevant NI/TI switchability. At present, laboratory synthesized 2D materials that are confirmed TIs include only graphene⁴ and silicene⁵ having, however, symmetry-enforced zero band gaps if spin–orbit coupling (SOC) is neglected, and

extremely small band gaps of $E_g = 10^{-3}$ meV and 1.55 meV, respectively, when the small SOC akin to such light elements is considered. Theoretically proposed but not laboratory realized hypothetical 2D TIs include “Stanene”,⁶ BiH,⁷ ZrTe₅, HfTe₅,⁸ and Bi₄Br₄⁹ that promise larger band gaps. However, it is not known if the structure assumed in these calculations to produce band inversion is thermodynamically realizable.¹⁰

One class of approaches to control Δ_{inv} in a single material family involves utilization of *structural or compositional degrees of freedom* such as alloying a NI with TI components,^{11,12} exerting quantum confinement on a NI quantum well by cladding it with a suitably chosen barrier material,^{13–16} or applying strain^{17–21} to a NI material attempting to induce thereby band inversion. However, controlling Δ_{inv} via such *material-intrinsic*, structural, or compositional knobs have limited flexibility as these approaches generally require different samples (e.g., different alloy compositions or different quantum well thicknesses) and, thus, (with the exception of strain) represent essentially discontinuous tuning. Such limitations would not be present if the control of Δ_{inv} and the ensuing topological invariant Z_2 would involve a *continuous external knob applied to a single, fixed material*. An example could be

Received: November 14, 2014

Revised: December 29, 2014

Published: January 21, 2015



applying an external electric field to a 2D NI material such that it transforms electronically into a TI. Such an integration of electric field engineering and topological quantum phases could effectively combine spin and charge transport under an electric field and, thus, could enable interesting physics and potential applications.²² However, although electrically controlled *insulator-to-metal* transition^{23–25} has been amply demonstrated in 2D systems (underlying the CMOS technology; proposed for spintronics), achievement of electrically controlled *normal-to-topological* transformation in 2D systems is rare.²⁶ Recently, such approach has been theoretically proposed for Sb_2Te_3 that is a TI in its bulk form (structure type $R\text{-}3m$). For thin layers containing up to four monolayers of Sb_2Te_3 segments (quintuple layer), first-principles calculations of Kim et al. predicted a transition from an NI to a TI under electric field.²⁶ Subsequent scanning tunneling microscopy (STM) measurement of surface state spectrum by Zhang et al. has verified the band gap tuning under low field, indicating the possibility for such topological phase transition.²⁷ However, Sb_2Te_3 is a high atomic-number material that is already a TI in bulk form, so in this case, the electric field effect did not change the fundamental, innate topological character of this compound.

Phosphorene is laboratory realized 2D material that can be made at various monolayer thicknesses by mechanical exfoliation of black phosphorus.^{28,29} The latter is a 3D elemental solid, a layered allotrope of white and red phosphorus that is thermodynamically stable in bulk form at room temperature and pressure. Phosphorene is a normal insulator with a sizable band gap (1.5–2.2 eV^{28,30–33}) for single-layer and positive inversion energy $\Delta_{\text{inv}} = E_g$. It is also predicted to have high-mobility at room temperature ($\sim 10^3 \text{ cm}^2 \text{ V}^{-1} \text{ s}^{-1}$), significant transport anisotropy within the 2D plane and linear dichroism.^{32,34–36} A field effect transistor (FET) action was indeed demonstrated in a few-layer phosphorene by manipulating the doping level via back-gate voltage,²⁹ leading to current modulation (on–off ratio) of the order of 10^5 . However, unlike other 2D monolayer elemental phases, such as graphene and silicene that are TIs, single-layer as well as few-layer phosphorene (until bulk) is an NI.

Using density functional theory (DFT) with electric field applied self-consistently to the stack of few-layer phosphorene, we predict that there will be a transition from a NI (positive Δ_{inv} and $Z_2 = 0$) to a TI (negative Δ_{inv} and $Z_2 = 1$) and eventually to a metal. Unlike Sb_2Te_3 , whose bulk form is already a TI, induced by the SOC of heavy atoms, here, black phosphorus is a low atomic-number NI at all thicknesses, so the prediction that this material can be converted to a TI by application of an electric field provides a totally field-induced phase transition and thus holds the potential of expanding the hitherto limited material base of TI by converting NI materials to TIs. The phase sequence is as follows: In the starting normal insulator phase, there is a direct band gap at the Brillouin zone center Γ , separating the unoccupied conduction band C1 from the occupied valence band V1. This insulating gap decreases monotonically as the electric field is applied. Beyond a critical field, which gets reduced as the stack gets thicker, a band inversion occurs whereby C1 becomes occupied and V1 becomes unoccupied and the calculated topological invariant (see below) becomes $Z_2 = 1$. Including the SOC, the Dirac-like band crossing becomes gapped, rendering the system a 2D TI with an occupied vs unoccupied band gap of 5 meV. Finally, at higher fields band C1 off Γ moves further down in energy and touches the Fermi level, and thus, the 2D system becomes

metallic while retaining the topological nontrivial feature. Such flexibly tuned phase transition would lead to spin-separated gapless edge states, that is, quantum spin Hall (QSH) effect, as well as normal insulating and conducting states. This prediction, building on the current FET technology, opens the possibility to make a *field effect topological transistor* that could manipulate both spin and charge carrier simultaneously.

Crystal Structure and Zero Field Electronic Structure of Few-Layer Phosphorene. Bulk black phosphorus (space group $Cmca$, D_{2h}^{18}) is a layered material in which individual atomic layers are bonded together by van der Waals interactions. Each P atom forms within its layer sp^3 -like hybridization by covalently bonding with the three adjacent P atoms, forming a buckled honeycomb structure, as shown in Figure 1a and b. Each monolayer consists of two P sublayers,

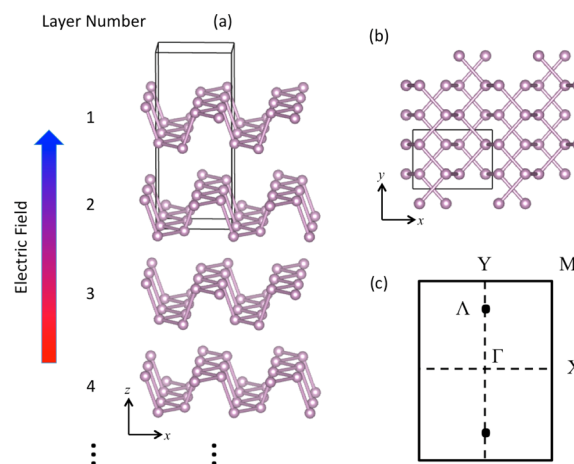


Figure 1. (a) Side view and (b) top view of the crystal structure of multilayer stack of phosphorene. The black frame indicates the unit cell of bulk black phosphorus. The electric field is applied along the stacking direction. (c) 2D first Brillouin zone.

and thus, the three P–P bonds can be classified as having two in-plane bonds within a sublayer plus an out-of-plane bond with another sublayer. Bulk 3D black phosphorus consisting of an infinite number of monolayers has lower DFT energy per phosphorene layer compared with finite layer stacks. Indeed, the “peeling energy” for an n -layer structure, that is, the energy change in going from 3D bulk to a finite n -layer structure $D(n) = (E(N) - E(N - n) - E(n))/n|_{N \rightarrow \infty}$ is around -60 meV/atom for $n = 1\text{--}4$, similar to the calculated counterpart of monolayer MoS_2 -73 meV/atom . This order of magnitude implies rather weak interlayer coupling³⁷ allowing practical peeling.

The band gap of *bulk* BP (measured 0.3 eV ³⁸) increases monotonically with decreasing number of layers n . Our DFT-PBE calculation (see Methods Section) reveals that the band gaps of $n = 4, 3, 2$, and 1 layers of phosphorene are all direct at Γ with $E_g = 0.07, 0.19, 0.42$, and 0.87 eV , respectively, in agreement with previous calculations based on the same method.^{32,39} In what follows, we use $n = 4$ layer phosphorene at PBE level. Figure 2a shows at zero field a normal insulator with a direct band gap located at Γ point. Both bands C1 and V1 exhibit sp^3 character of P atom but differ in their symmetric representations at the Γ point (point group D_{2h}): band C1 (blue) has the representation $A_g(\Gamma_1)$, whereas band V1 (red) has the representation $B_{3u}(\Gamma_8)$ that is antisymmetric with respect to the operators including inversion, C_{2y} and C_{2z} of 2-

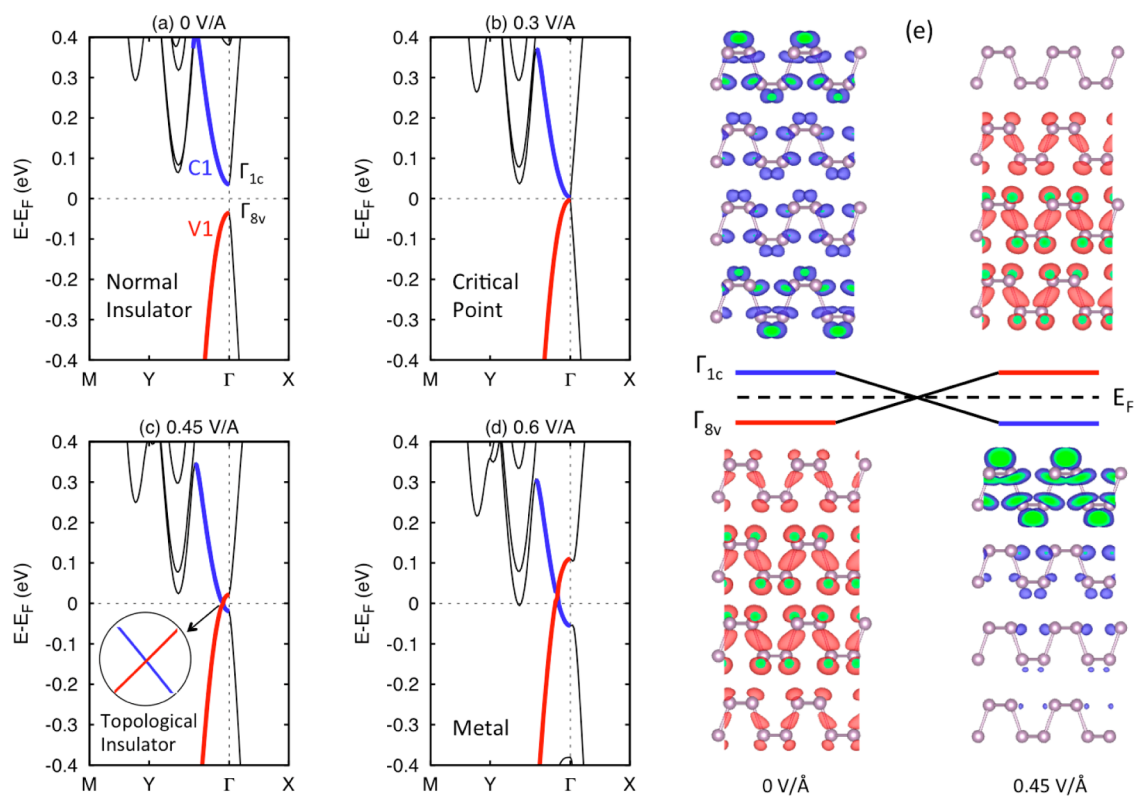


Figure 2. (a)–(d) Band structures of 4-layer phosphorene with an external electric field of (a) 0 V/Å, (b) 0.3 V/Å, (c) 0.45 V/Å, and (d) 0.6 V/Å on PBE level. SOC is not included. The V1 and C1 states are highlighted by red and blue, respectively. (e) Band evolution of Γ_{1c} and Γ_{8v} before (0 V/Å) and after (0.45 V/Å) electric field with the corresponding magnitude of squared wave function of 4-layer phosphorene. Purple balls denote the phosphorus atoms. The amplitude of isosurface is 0.03 au.

fold rotation axis. In addition, the band dispersion along the k_x and k_y direction shows strong anisotropy (see the 2D rectangular Brillouin zone in Figure 1c). The effective mass along Γ – X is much lower than that along Γ – Y because of the preference of bonding direction along x direction,³² as shown in Figure 1a. The topological invariant at zero field is $Z_2 = 0$, confirming that few-layer phosphorene is a NI.

From NI to TI: Band Gap Closure and Band Inversion.

We search for the topological phase transition by applying an external field F_{\perp} to the n -layer stack for $n = 1$ –4. In order to understand the main effects of the electric field we first exclude SOC in the calculation. Due to the Stark effect, the energy shift caused by the difference of electrostatic potential between different layers can be approximately expressed as $\Delta E = -F^*ed$, where F^* is the screened electric field and d is the interlayer distance. In order to monitor the band inversion, we define the inversion energy as $\Delta_{inv} = E_{\Gamma_{1c}} - E_{\Gamma_{8v}}$ (see Figure 2a). With F_{\perp} increasing, the band gap E_g decreases monotonically, and so does Δ_{inv} , until a critical field $F_c = 0.3$ V/Å. At this field band V1 and band C1 touch at Γ , as shown in Figure 2b. For $F_{\perp} > F_c$, the band gap E_g remains zero but Δ_{inv} becomes negative. This band inversion is induced entirely by the field F_{\perp} rather than by SOC. Similar proposals in which band inversion is induced by factors other than SOC appear in ZrTe_5 and HfTe_5 ,⁸ GaS and GaSe ,¹⁸ graphene-like materials.^{4–6}

The schematic diagram of the evolution of energy level Γ_{1c} and Γ_{8v} , accompanied by the corresponding magnitude of squared wave function is shown in Figure 2e. At zero field, the atomic orbitals of Γ_{8v} (red, occupied at zero field) are distributed along the out-of-plane bonds of two P sublayers but are antisymmetric along the in-plane bonds within each P

sublayer. In contrast, atomic orbitals of Γ_{1c} (blue, unoccupied at zero field) have nodes in the out-of-plane bonds while being symmetric along the in-plane bonds. Once the electric field exceeds F_c , we find that the Γ_{1c} state is now occupied and the Γ_{8v} state is empty, indicating a band inversion with negative Δ_{inv} . Although the charge density tends to aggregate at the side layer because of the electrostatic potential and thus inversion symmetry is broken, the rotation symmetry with respect to C_{2z} 2-fold axis still differs Γ_{8v} and Γ_{1c} by group representation (actually, Γ_{8v} state becomes Γ_{2v} after applying field because the symmetry of Γ is lowered). This band inversion at Γ ensures a nontrivial topological invariant $Z_2 = 1$ and, thus, achieve the topological phase transition tuned by F_{\perp} .

Figure 3a shows the inversion energy Δ_{inv} at Γ of $n = 2$ -, 3-, and 4-layer phosphorene as a function of the electric field. For $n = 2$ layer, there is no phase transition within our field range (same case for monolayer phosphorene) because the zero-field gap is large. On the other hand, for both $n = 3$ - and 4-layer phosphorene, we detect phase transition with the critical field of 0.55 V/Å and 0.3 V/Å, respectively. The result Δ_{inv} vs F_{\perp} of 4-layer phosphorene considering SOC effect is also shown in Figure 3a. We find that the SOC effect in light atom P is weak, so it does not affect much the inversion energy at Γ as well as the critical field F_c .

The discussion above pertains to band inversion at Γ , not at the other time reversal invariant momenta (TRIM). The quantity that captures the full topological response over the TRIMs is the Z_2 invariant. For few-layer phosphorene under electric fields, the calculation of Z_2 invariant is not as straightforward as that under zero field because finite field breaks the inversion symmetry, which means the regular

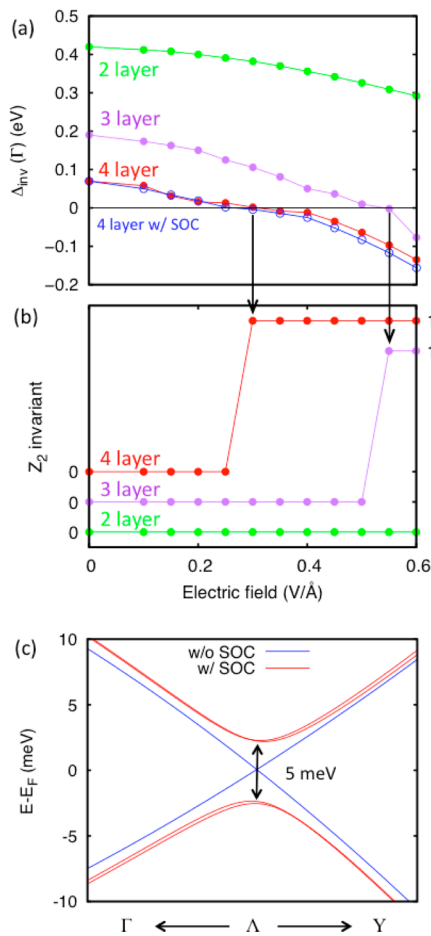


Figure 3. (a) Inversion energy Δ_{inv} (PBE level) of 2-, 3-, and 4-layer phosphorene at Γ point as a function of the electric field. The negative values indicate nontrivial topological phases. SOC is not included unless specified in 4-layer phosphorene. (b) Z_2 invariant of 2, 3, and 4-layer phosphorene. SOC is included throughout the calculation. It is shown in both panels that for 3- and 4-layer phosphorene, the critical field for the phase transition is 0.55 V/Å and 0.3 V/Å, respectively. (c) Graphene-like band structure of 4-layer phosphorene in the vicinity of Λ point with (red) and without (blue) SOC.

method that evaluates the band parity¹ does not apply. Here, we use a more general method by Fu and Kane.⁴⁰ For solids that have time-reversal symmetry, the time reversal operator matrix relates time reversed wave functions by

$$B_{\alpha\beta}(K_i) = \langle u_{-K_i, \alpha} | \Theta | u_{K_i, \beta} \rangle \quad (1)$$

where $u_{K_i, \alpha}$ is the Bloch wave function for occupied band α at TRIM K and Θ is the time-reversal operator. At TRIM K_i where the Hamiltonian commutes with the time-reversal operator, $B(K_i)$ is antisymmetric. Its Pfaffian, whose square is equal to the determinant, may characterize an antisymmetric matrix. Then $\delta(K_i) = (\det[B(K_i)])^{1/2} / (P_i[B(K_i)])$ can take ± 1 values. The distribution of all values of $\{\delta(K_i)\}$ will be used below to classify different topological types. Therefore, Z_2 is defined as

$$(-1)^{Z_2} = \prod_i \delta(K_i) \quad (2)$$

Figure 3b shows the evolution of Z_2 invariant of 2-, 3-, and 4-layer phosphorene with respect to F_{\perp} . We note that for 3- and 4-layer phosphorene, the jumping point of Z_2 exactly correlates to the critical field of Δ_{inv} , which means that it is the band

inversion at Γ induced by F_{\perp} causing the topological phase transition.

Graphene-Like Dirac Cones. Ignoring SOC, when the field $F_{\perp} > F_c$, the band inversion at Γ is accompanied by a Dirac-like band crossing along $\Gamma - Y$. Figure 2c suggests that along $\Gamma - Y$ the band crossing induced by V1 and C1 ensures few-layer phosphorene semimetals with two nodes $\Lambda(0, \pm y_D)$ at the Fermi level (also see Figure 1c). This band crossing is protected by fractional translation symmetry due to the different band character of the two bands (red and blue in Figure 2c). Therefore, they are describable by two 2×2 Dirac equations, similar to the “massless Dirac Fermions” in graphene and silicene without SOC. This band crossing further implies the band inversion on different sides of Λ , that is, Γ and Y , and confirms that the band inversion is totally induced by the electric field, rather than by SOC. With F_{\perp} increasing, V1 and C1 continuously shift upward and downward, respectively. As a result, the Dirac cone red shifts toward Y point (see Figure 2d). On the other hand, along $\Gamma - X$, there is no band crossing because of the absence of fractional translation symmetry along this high-symmetry line, also indicating the anisotropy between x and y direction.

The SOC in P is too weak to affect the band inversion. However, it lifts the degeneracy at the Dirac point Λ and, thus, opens a gap at the Fermi level, as shown in Figure 3c. Therefore, the electronic behavior of few-layer phosphorene under field is quite similar to graphene-like 2D structures, as “Dirac semimetals” without SOC and 2D TIs with SOC.^{5,41} The band gap of 4-layer phosphorene under 0.45 V/Å is about 5 meV, much larger than that of its 2D elemental counterpart graphene and silicene (10^{-3} meV and 1.55 meV, respectively). The band gap opening could be interpreted by the evolution of band symmetry. Under zero field, V1 and C1 at Λ belong to different single group irreducible representations under fractional translation operation. When electric field and SOC are both applied, the inversion symmetry is removed and the Λ symmetry is reduced. As a result, V1 and C1 have the same irreducible representation and thus an anticrossing rather than crossing. We note that unlike graphene-like materials, in phosphorene inversion symmetry breaking (by applying electric field) is needed to open the SOC-induced gap. This is because compared with graphene, few-layer phosphorene has a nonsymmorphic space group containing fractional translations that protect the symmetry difference between V1 and C1. In addition, because the inversion symmetry is broken under electric field, there is spin splitting at the non-time-reversal invariant Λ point, as shown in Figure 3c (similar to the Rashba effect at the K valley in gated graphene and silicene^{42,43}).

From TI to (Topological) Metal: Possible Implications on Field Effect Topological Transistor. Above the critical field, increasing the electric field would enhance the reopened gap at Γ (absolute value of Δ_{inv}), keeping the topological nontrivial phase of few-layer phosphorene. As long as few-layer phosphorene in the TI phase, the QSH effect should be realized.^{2,4} On the other hand, when the electric field reaches another critical field value of $F_M = 0.6$ V/Å, as shown in Figure 2d, we find that another valley of C1 approaches the Fermi level, and thus the system becomes metallic. However, this phase transition does not affect the inverted bands at Γ and, thus, the topological character. This is verified by our calculation of the Z_2 invariant. Therefore, the phase transition sequence of few-layer phosphorene under increased electric field is “NI—TI—topological metal”. Such phase transition

provides the possibility to construct a “field effect topological transistor (FETT)” by applying different gate voltages. Here, we propose a dual-gated FETT model composed of few-layer phosphorene as the channel, as shown in Figure 4a. Compared

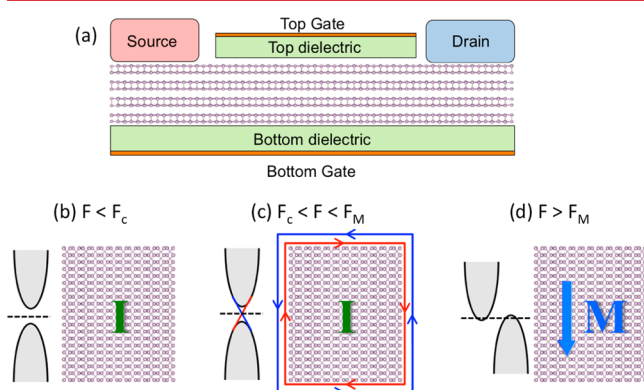


Figure 4. (a) Model of a dual-gated topological field effect transistor based on a few-layer phosphorene channel. (b–d) Schematic band structure and spin and charge current in the phosphorene channel for (b) $F < F_c$, (c) $F_c < F < F_M$ and (d) $F > F_M$. The letter “I” and “M” stands for insulating and metallic, respectively.

with single gate, a dual-gated device can tune not only the perpendicular electric field working on the channel but also the Fermi level.⁴⁴ Figure 4b–d explains the phase transition and the corresponding spin and charge current on the channel. When $F < F_c$, the FETT performs as “OFF” state because the phosphorene channel remains a normal insulator. When $F > F_M$, The FETT is switched to “ON” state, with the charge current flowing through the entire 2D sheet. Finally, as F falls between two critical fields F_c of and F_M , a topological nontrivial “QSH” state occurs, with the 2D sheet remaining insulating but net spin current on the edge of the channel. The spin-up and spin-down electrons propagate oppositely, resilient to nonmagnetic chemical passivation (like H termination) and to normal backscattering.

We note that if such a FETT could be switched between “ON” and “OFF” state, that is, intrinsically metallic or insulating, there must be “QSH” phase between them. As previously discussed, the nontrivial band gap is 5 meV, much larger than that of its 2D elemental counterpart graphene and silicene. However, it still requires a relative low temperature (<58 K) to realize the QSH effect. It is because when the decreasing Δ_{inv} approaches $k_B T$ before critical field, electrons begin to transition thermodynamically, and thus, the insulator phase will directly jumps to metal phase without passing through TI phase. Therefore, given that the range of electric field that brings few-layer phosphorene to TI is achievable (e.g., 0.3–0.6 V/Å for 4-layer phosphorene), we expect the oppositely propagating spin current to be verified in a reasonable experimental setup.

Manipulating the Required Critical Field. Because the PBE exchange correlation often underestimates the band gap, we have also used the more accurate hybrid functional (HSE06). The HSE band gap of 4-layer phosphorene under zero field is 0.65 eV, which is considerably larger than the PBE result of 0.07 eV and in agreement with previous calculations on the same level.^{32,39} As a result, the critical field increases from 0.3 V/Å (PBE level) to 0.7 V/Å (HSE level). On the other hand, the decreasing trend of band gap versus electric

field remains unchanged under HSE functional. Furthermore, the band symmetry of V1 and C1 only depend on the critical field, but not the exchange functional we choose, indicating that the NI–TI transition is still robust but requires larger field. In monolayer phosphorene, the quasiparticle band gap calculated by many-body approach (G_0W_0) reveals a larger gap (2.0–2.2 eV)³¹ compared with HSE results (~ 1.5 eV). Such a band gap is recently observed by scanning tunneling spectroscopy (2.0 eV)³³ and photoluminescence excitation spectroscopy (2.2 eV).³⁰ Therefore, the critical electric field for the topological transition of few-layer phosphorene could be even larger than the results of HSE.

It is both interesting and practical to discuss ways of reducing this value of critical field. In order to realize the topological phase transition, one could increase the number of layers n of phosphorene to get a smaller critical field. It is because (i) the band gap decreases with the layer number, approaching the bulk value (~ 0.3 eV). In the proposed FET made by few-layer phosphorene, the thickness of the sample with good quality lies in the range of 5–10 nm, corresponding 10–20 layers of phosphorene.²⁹ By extrapolating HSE06 band gaps of such a thickness, we estimate the band gap is within 0.30–0.35 eV. (ii) Due to the Stark effect, the response to electric field becomes more significant with thicker layers. In addition, the band edges still locate at Γ for thicker phosphorene slab until bulk state,²⁹ indicating that the TI phase would appear before the metal phase by applying electric field (assuming a rigid band shift). Therefore, considering the compromise of computational cost, we choose PBE calculations that underestimate the critical field and four layers whose E_c can be optimized by simply adding the phosphorene layers to schematically prove the topological phase transition.

Considerations for Other 2D Materials That Could Have Electrical-Induced NI-to-TI Topological Transition.

On the basis of the calculations above, one could enquire what are the necessary general conditions for materials that would manifest an electric field induced conversion of a 2D NI to a TI. First, one should be able to close the band by applying a reasonable field. Second, such material needs to have a direct band gap located at a TRIM (for the tetragonal Brillouin zone these are Γ , X, Y, and M) because if the band gap were to occur at non-TRIM then either an indirect band gap or direct band gap would make the metal phase occur before the topological band inversion. Considering all the four TRIMs, the degeneracy of valleys should be an odd number. For example, if the direct gap is located at the X point in a square lattice, the band inversion will still lead to $Z_2 = 0$ because the X valley is doubly degenerate.⁴⁵ Third, after the inversion symmetry is broken by the electric field, the band edge k -point of V1 and C1 should have different band character (group representation) to make the band inversion nontrivial. Finally, away from the TRIM where band inversion takes place, V1 and C1 should have the same band character to avoid a band crossing and, thus, keep the gated system an insulator. With respect to these design principles, few-layer phosphorene is different that some of the other well-known 2D systems such as transition metal dichalcogenides, graphene, and its analogs.

Conclusion and Discussion. Recently, Zhang et al. has proposed and observed an *insulating-to-metallic* transfer curve in phosphorene by sweeping the single-gate voltage.²⁹ Here, we add a crucial ingredient, predicting that in few-layer phosphorene there will be a normal-to-topological phase transition induced purely by applying an electric field and occurring before the

system becomes intrinsically metallic. The topological band inversion originates entirely from the field-induced Stark effect, whereas the effect of SOC is to open an energy gap at the Dirac-like band crossing, rendering the system a 2D TI. This topological nontrivial feature persists after the system becomes metallic at higher fields. Such tunable phase transition could lead to spin-separated gapless edge states, that is, quantum spin Hall effect, which is easy to detect as well as normal insulating and conducting states based on the current FET technology. This finding opens the possibility of making a multifunctional “field effect topological transistor” that could manipulate simultaneously both spins and charge carrier.

Methods. The calculations were performed with the Vienna *ab initio* package (VASP).⁴⁶ The geometrical and electronic structures are calculated by the projector-augmented wave (PAW) pseudopotential⁴⁷ and the generalized gradient approximation of Perdew, Burke, and Ernzerhof (PBE)⁴⁸ to the exchange-correlation functional unless specified. Electronic structures calculated by hybrid functional (HSE06)⁴⁹ is also provided for comparison. Spin-orbit coupling is calculated by a perturbation $\sum_{i,l,m} V_i^{SO} \vec{L} \cdot \vec{S}|l,m\rangle_i \langle l,m|$ to the pseudopotential, where $|l,m\rangle_i$ is the angular momentum eigenstate of *i*th atomic site.⁵⁰ The plane wave energy cutoff is set to 550 eV, and the electronic energy minimization was performed with a tolerance of 10^{-4} eV. All the lattice parameters and atomic positions were fully relaxed with a tolerance of 10^{-3} eV/Å. The van der Waals interaction is considered by a dispersion-corrected PBE-D2 method.⁵¹ The vacuum separation in the slab supercell is 20 Å to avoid the interaction between periodic images.

The electric field can be featured as an additional sawtooth potential along the *z* direction with discontinuity at the mid plane of the vacuum region of the supercell. The automatic symmetry constraint in VASP is switched off to avoid the incorrect rendering of the electric field.⁴⁴ To test the general correctness of the critical field, we also use Quantum Espresso⁵² as comparison and find that the dependence of the band gap on the electric field agrees well with the results of VASP.

AUTHOR INFORMATION

Corresponding Authors

*E-mail: qihang.liu85@gmail.com.

*E-mail: alex.zunger@colorado.edu.

Notes

The authors declare no competing financial interest.

ACKNOWLEDGMENTS

This work was supported by NSF Grant titled “Theory-Guided Experimental Search of Designed Topological Insulators and Band-Inverted Insulators” (no. DMREF-13-34170). This work used the Extreme Science and Engineering Discovery Environment (XSEDE), which is supported by National Science Foundation grant number ACI-1053575.

REFERENCES

- (1) Fu, L.; Kane, C. L. *Phys. Rev. B* **2007**, *76*, 045302.
- (2) Qi, X.-L.; Zhang, S.-C. *Rev. Mod. Phys.* **2011**, *83*, 1057–1110.
- (3) Hasan, M. Z.; Kane, C. L. *Rev. Mod. Phys.* **2010**, *82*, 3045–3067.
- (4) Kane, C. L.; Mele, E. J. *Phys. Rev. Lett.* **2005**, *95*, 226801.
- (5) Liu, C.-C.; Feng, W.; Yao, Y. *Phys. Rev. Lett.* **2011**, *107*, 076802.
- (6) Xu, Y.; Yan, B.; Zhang, H.-J.; Wang, J.; Xu, G.; Tang, P.; Duan, W.; Zhang, S.-C. *Phys. Rev. Lett.* **2013**, *111*, 136804.
- (7) Song, Z.; Liu, C.-C.; Yang, J.; Han, J.; Ye, M.; Fu, B.; Yang, Y.; Niu, Q.; Lu, J.; Yao, Y. *NPG Asia Mater.* **2014**, *6*, e147.

- (8) Weng, H.; Dai, X.; Fang, Z. *Phys. Rev. X* **2014**, *4*, 011002.
- (9) Zhou, J.-J.; Feng, W.; Liu, C.-C.; Guan, S.; Yao, Y. *Nano Lett.* **2014**, *14*, 4767–4771.
- (10) Trimarchi, G.; Zhang, X.; Freeman, A. J.; Zunger. *Phys. Rev. B* **2014**, *90*, 161111(R).
- (11) Hsieh, D.; Xia, Y.; Wray, L.; Qian, D.; Pal, A.; Dil, J. H.; Osterwalder, J.; Meier, F.; Bihlmayer, G.; Kane, C. L.; Hor, Y. S.; Cava, R. J.; Hasan, M. Z. *Science* **2009**, *323*, 919–922.
- (12) Hsieh, D.; Xia, Y.; Qian, D.; Wray, L.; Dil, J. H.; Meier, F.; Osterwalder, J.; Patthey, L.; Checkelsky, J. G.; Ong, N. P.; Fedorov, A. V.; Lin, H.; Bansil, A.; Grauer, D.; Hor, Y. S.; Cava, R. J.; Hasan, M. Z. *Nature* **2009**, *460*, 1101–1105.
- (13) Zhang, D.; Lou, W.; Miao, M.; Zhang, S.-c.; Chang, K. *Phys. Rev. Lett.* **2013**, *111*, 156402.
- (14) Miao, M. S.; Yan, Q.; Van de Walle, C. G.; Lou, W. K.; Li, L. L.; Chang, K. *Phys. Rev. Lett.* **2012**, *109*, 186803.
- (15) Knez, I.; Du, R.-R.; Sullivan, G. *Phys. Rev. Lett.* **2011**, *107*, 136603.
- (16) König, M.; Wiedmann, S.; Brüne, C.; Roth, A.; Buhmann, H.; Molenkamp, L. W.; Qi, X.-L.; Zhang, S.-C. *Science* **2007**, *318*, 766–770.
- (17) Liu, Y.; Li, Y. Y.; Rajput, S.; Gilks, D.; Lari, L.; Galindo, P. L.; Weinert, M.; Lazarov, V. K.; Li, L. *Nat. Phys.* **2014**, *10*, 294–299.
- (18) Zhu, Z.; Cheng, Y.; Schwingenschlögl, U. *Phys. Rev. Lett.* **2012**, *108*, 266805.
- (19) Feng, W.; Zhu, W.; Weitering, H. H.; Stocks, G. M.; Yao, Y.; Xiao, D. *Phys. Rev. B* **2012**, *85*, 195114.
- (20) Young, S. M.; Chowdhury, S.; Walter, E. J.; Mele, E. J.; Kane, C. L.; Rappe, A. M. *Phys. Rev. B* **2011**, *84*, 085106.
- (21) Guinea, F.; Katsnelson, M. I.; Geim, A. K. *Nat. Phys.* **2010**, *6*, 30–33.
- (22) Liu, J.; Hsieh, T. H.; Wei, P.; Duan, W.; Moodera, J.; Fu, L. *Nat. Mater.* **2014**, *13*, 178–183.
- (23) Radisavljevic, B.; Radenovic, A.; Brivio, J.; Giacometti, V.; Kis, A. *Nat. Nano* **2011**, *6*, 147–150.
- (24) Schwierz, F. *Nat. Nano* **2010**, *5*, 487–496.
- (25) Zhang, Y.; Tang, T.-T.; Girit, C.; Hao, Z.; Martin, M. C.; Zettl, A.; Crommie, M. F.; Shen, Y. R.; Wang, F. *Nature* **2009**, *459*, 820–823.
- (26) Kim, M.; Kim, C. H.; Kim, H.-S.; Ihm, J. *Proc. Natl. Acad. Sci. U.S.A.* **2012**, *109*, 671–674.
- (27) Zhang, T.; Ha, J.; Levy, N.; Kuk, Y.; Stroscio, J. *Phys. Rev. Lett.* **2013**, *111*, 056803.
- (28) Liu, H.; Neal, A. T.; Zhu, Z.; Luo, Z.; Xu, X.; Tománek, D.; Ye, P. D. *ACS Nano* **2014**, *8*, 4033–4041.
- (29) Li, L.; Yu, Y.; Ye, G. J.; Ge, Q.; Ou, X.; Wu, H.; Feng, D.; Chen, X. H.; Zhang, Y. *Nat. Nano* **2014**, *9*, 372–377.
- (30) Wang, X.; Jones, A. M.; Seyler, K. L.; Tran, V.; Jia, Y.; Zhao, H.; Wang, H.; Yang, L.; Xu, X.; Xia, F. Highly Anisotropic and Robust Excitons in Monolayer Black Phosphorus. 2014, *arXiv:1411.1695*. arXiv.org e-Print archive. <http://arxiv.org/abs/1411.1695> (accessed December 2014).
- (31) Tran, V.; Soklaski, R.; Liang, Y.; Yang, L. *Phys. Rev. B* **2014**, *89*, 235319.
- (32) Qiao, J.; Kong, X.; Hu, Z.-X.; Yang, F.; Ji, W. *Nat. Commun.* **2014**, *5*, 4475.
- (33) Liang, L.; Wang, J.; Lin, W.; Sumpter, B. G.; Meunier, V.; Pan, M. *Nano Lett.* **2014**, *14*, 6400–6406.
- (34) Fei, R.; Yang, L. *Nano Lett.* **2014**, *14*, 2884–2889.
- (35) Rodin, A. S.; Carvalho, A.; Castro Neto, A. H. *Phys. Rev. Lett.* **2014**, *112*, 176801.
- (36) Xia, F.; Wang, H.; Jia, Y. *Nat. Commun.* **2014**, *5*, 4458.
- (37) Ataca, C.; Şahin, H.; Ciraci, S. *J. Phys. Chem. C* **2012**, *116*, 8983–8999.
- (38) Keyes, R. W. *Phys. Rev.* **1953**, *92*, 580–584.
- (39) Guo, H.; Lu, N.; Dai, J.; Wu, X.; Zeng, X. C. *J. Phys. Chem. C* **2014**, *118*, 14051–14059.
- (40) Fu, L.; Kane, C. L. *Phys. Rev. B* **2006**, *74*, 195312.

- (41) Yao, Y.; Ye, F.; Qi, X.-L.; Zhang, S.-C.; Fang, Z. *Phys. Rev. B* **2007**, *75*, 041401.
- (42) Abdelouahed, S.; Ernst, A.; Henk, J.; Maznichenko, I. V.; Mertig, I. *Phys. Rev. B* **2010**, *82*, 125424.
- (43) Tsai, W.-F.; Huang, C.-Y.; Chang, T.-R.; Lin, H.; Jeng, H.-T.; Bansil, A. *Nat. Commun.* **2013**, *4*, 1500.
- (44) Liu, Q.; Li, L.; Li, Y.; Gao, Z.; Chen, Z.; Lu, J. *J. Phys. Chem. C* **2012**, *116*, 21556–21562.
- (45) Slager, R.-J.; Mesáros, A.; Juricic, V.; Zaanen, J. *Nat. Phys.* **2013**, *9*, 98–102.
- (46) Kresse, G.; Furthmüller, J. *Comput. Mater. Sci.* **1996**, *6*, 15–50.
- (47) Kresse, G.; Joubert, D. *Phys. Rev. B* **1999**, *59*, 1758–1775.
- (48) Perdew, J. P.; Burke, K.; Ernzerhof, M. *Phys. Rev. Lett.* **1996**, *77*, 3865–3868.
- (49) Heyd, J.; Scuseria, G. E.; Ernzerhof, M. *J. Chem. Phys.* **2003**, *118*, 8207–8215.
- (50) Bloński, P.; Hafner, J. *Phys. Rev. B* **2009**, *79*, 224418.
- (51) Grimme, S. *J. Comput. Chem.* **2006**, *27*, 1787–1799.
- (52) Paolo, G.; Stefano, B.; Nicola, B.; Matteo, C.; Roberto, C.; Carlo, C.; Davide, C.; Guido, L. C.; Matteo, C.; Ismaila, D.; Andrea Dal, C.; Stefano de, G.; Stefano, F.; Guido, F.; Ralph, G.; Uwe, G.; Christos, G.; Anton, K.; Michele, L.; Layla, M.-S.; Nicola, M.; Francesco, M.; Riccardo, M.; Stefano, P.; Alfredo, P.; Lorenzo, P.; Carlo, S.; Sandro, S.; Gabriele, S.; Ari, P. S.; Alexander, S.; Paolo, U.; Renata, M. W. *J. Phys.: Condens. Matter* **2009**, *21*, 395502.